

Characterization of the Wind Power Resource in Europe and its Intermittency

Alexandra Cosserson, C. Adam Schlosser and U. Bhaskar Gunturu



Report No. 258
March 2014

The MIT Joint Program on the Science and Policy of Global Change is an organization for research, independent policy analysis, and public education in global environmental change. It seeks to provide leadership in understanding scientific, economic, and ecological aspects of this difficult issue, and combining them into policy assessments that serve the needs of ongoing national and international discussions. To this end, the Program brings together an interdisciplinary group from two established research centers at MIT: the Center for Global Change Science (CGCS) and the Center for Energy and Environmental Policy Research (CEEPR). These two centers bridge many key areas of the needed intellectual work, and additional essential areas are covered by other MIT departments, by collaboration with the Ecosystems Center of the Marine Biology Laboratory (MBL) at Woods Hole, and by short- and long-term visitors to the Program. The Program involves sponsorship and active participation by industry, government, and non-profit organizations.

To inform processes of policy development and implementation, climate change research needs to focus on improving the prediction of those variables that are most relevant to economic, social, and environmental effects. In turn, the greenhouse gas and atmospheric aerosol assumptions underlying climate analysis need to be related to the economic, technological, and political forces that drive emissions, and to the results of international agreements and mitigation. Further, assessments of possible societal and ecosystem impacts, and analysis of mitigation strategies, need to be based on realistic evaluation of the uncertainties of climate science.

This report is one of a series intended to communicate research results and improve public understanding of climate issues, thereby contributing to informed debate about the climate issue, the uncertainties, and the economic and social implications of policy alternatives. Titles in the Report Series to date are listed on the inside back cover.

Ronald G. Prinn and John M. Reilly
Program Co-Directors

For more information, please contact the Joint Program Office

Postal Address: Joint Program on the Science and Policy of Global Change
77 Massachusetts Avenue
MIT E19-411
Cambridge MA 02139-4307 (USA)

Location: 400 Main Street, Cambridge
Building E19, Room 411
Massachusetts Institute of Technology

Access: Phone: +1.617. 253.7492
Fax: +1.617.253.9845
E-mail: globalchange@mit.edu
Web site: <http://globalchange.mit.edu/>

Characterization of the Wind Power Resource in Europe and its Intermittency

Alexandra Cosseron^{*†}, C. Adam Schlosser[‡], and Udaya Bhaskar Gunturu

Abstract

Wind power is assessed over Europe, with special attention given to the quantification of intermittency. Using the methodology developed in Gunturu and Schlosser (2011), the MERRA boundary flux data was used to compute wind power density profiles over Europe. Besides of the analysis of capacity factor, other metrics are presented to further quantify the availability and reliability of this resource and the extent to which wind-power intermittency is coincident across Europe. The analyses find that, consistent with previous studies, the majority of European wind power resources are located offshore. The largest wind power resources at onshore locations are found to be over Iceland, the United Kingdom, and along the northern coastlines of continental Europe. Other isolated pockets of higher wind power are found over Spain and along the Mediterranean coast of France. Overall, the availability of onshore wind power is low and is highly intermittent, while offshore locations show a high degree of persistence. However, for the strongest onshore locations of wind power—primarily over northern coastlines as well as the United Kingdom and Iceland—the evidence indicates that intermittency can be reduced by aggregation and interconnection of wind-power installations.

Contents

1. INTRODUCTION.....	2
2. METHODOLOGY	3
2.1 Data	3
2.2 Wind Power Density.....	3
3. CHARACTERIZATION OF WIND POWER RESOURCE	5
3.1 Descriptive Statistics of Wind Power	5
3.1.1 Mean and Median WPD	5
3.1.2 Coefficient of Variation of Wind Power.....	6
3.1.3 Interquartile Range.....	7
4. WIND DATA ASSESSMENT AND COMPARISON WITH PREVIOUS STUDIES.....	8
4.1 Comparison with Archer (2005).....	8
4.2 Comparison with EEA Report.....	9
4.3 Comparison with Risø National Laboratory Assessment	11
5. FURTHER ASSESSMENT OF THE WIND POWER RESOURCE	15
5.1 Availability of Wind Power.....	16
5.3 Distinction between Variability and Intermittency	19
5.4 Wind Episodes Lengths.....	19
5.5 Spatial Coincidence of Intermittency	21
5.5.1 AntiCoincidence.....	22
5.5.3 AntiNullCoincidence	23
6. WIND POWER RESOURCE AT DIFFERENT HUB HEIGHTS	25
6.1 Wind Power Density at various hub heights.....	25
6.2 Episode Length at Different Hub Heights	26
7. CONCLUSION	28
REFERENCES.....	29

* Ecole des Mines de Paris—Ecole Polytechnique, Paris, France.: alexandra.cosseron@polytechnique.org;

† Corresponding author (email: alexandra.cosseron@polytechnique.org).

‡ Joint Program on the Science and Policy of Global Change, Massachusetts Institute of Technology, Cambridge, MA, USA.

1. INTRODUCTION

Europe has seen a heightened interest in renewable energy over the last several years, especially in wind energy and quantified assessments of this resource as well as its reliability. The European Commission recently defined goals for the member states of the European Union (EU) in terms of renewables. EU leaders set targets in 2007 to move toward a highly energy-efficient, low-carbon economy, and then enacted them through the climate and energy package signed in 2009 (Directive 2009/28/EC, 2009). It states that the EU must achieve the “three twenties” by 2020: raising the share of EU energy consumption produced from renewable resources to 20%; a 20% reduction in European greenhouse gas emissions from 1990 levels; and a 20% improvement in the EU energy efficiency. The first criterion is the most well defined. Each member state was assigned a target percentage to be reached by 2020 in order to achieve the global objective at the EU level. For instance, this target percentage is 23% for France. These percentages tried to reflect the current levels of renewables in each member state and the economic wellbeing of the country in order to set reachable goals for everyone.

Wind power will be an important generation technology as part of any renewable energy portfolio deployment strategy. It is therefore critical to provide quantitative assessments as to where the largest resources exist. Moreover, wind power is an intermittent resource and there is an increasing awareness that this intermittency under large-scale deployment scenarios may undermine its potential for reliable generation. This further underscores the importance of diagnostic studies that provide actionable information for strategic generation deployments as well as infrastructure to optimize power availability. In previous studies, many researchers used data from meteorological towers or observations from airports. Most of these observations are at different heights and different schemes and have been used to extrapolate the wind speeds to the wind turbine hub heights. Kiss (2008) used the ECMWF’s ERA-40 (European Centre for Medium-Range Weather Forecasts’ 44-year reanalysis) eastward and northward winds at 10 m, that covers a time period of 44 years, from September 1, 1958 to August 31, 2002, in order to study wind field statistics over Europe. Larsen (2009) also used reanalysis data from NCEP/NCAR (National Center for Environmental Prediction/National Center for Atmospheric Research) to estimate the geostrophic wind and extrapolated the geostrophic wind to 10 m height. Archer (2007) used upper air measurements from balloons and rawinsondes at the nearest meteorological stations to extrapolate wind speeds at 10 m to the hub height at 50 m or 80 m. Similarly, many researchers used a power or logarithmic law assuming roughness length and friction velocity in the boundary layer that did not vary with seasons, terrain and stability of the atmosphere.

Recently, Cox (2009) noted the importance of modeling wind farm outputs as well as a comprehensive understanding of historical wind patterns at all the locations where wind farms are likely to be built. In addition, any data employed in such assessments must employ the highest temporal resolution (i.e. hours or shorter), such that robust historical correlations between different locations can be calculated and extrapolated to a hub height of interest.

This report provides a multidecadal (1979–2009) assessment of the wind power resource over Europe, following a methodology developed by Gunturu and Schlosser (2011). Wind power densities (WPDs) are computed from the MERRA (Modern-Era Retrospective Analysis for Research and Applications) data product, which we describe in the next section. The methodology of the WPD metric as well as other diagnostics regarding its intermittency, variability and capacity factor mapping are also provided. We present results of our analyses in Sections 3 to 6 and provide closing remarks in Section 7.

2. METHODOLOGY

2.1 Data

We employ the MERRA reanalysis data of Rienecker et al. (2011) that has a spatial resolution of $1/2^\circ \times 2/3^\circ$ and a temporal hourly resolution that spans 31 years (1979–2009). Specifically, the variables required for this analysis are: air density, displacement height, friction velocity, and roughness length. MERRA reconstructs the atmospheric state by assimilating observational data from different platforms into a global model. The MERRA database has been constructed with GEOS-5 ADAS—Atmospheric Data Assimilation System—version 5.2.0. The system consists of the GEOS-5 model and the Gridpoint Statistical Interpolation (GSI) analysis. GSI is a system developed jointly by the Global Modeling and Assimilation Office (GMAO) and the National Oceanic and Atmospheric Administration's National Centers for Environmental Prediction (NOAA/NCEP). The data assimilation includes conventional data from many sources as well as data from several trains of satellites. MERRA was constructed at the NASA Center for Climate Simulation as three separate analysis streams and aimed at providing a more accurate data set using the comprehensive suite of satellite based information for climate and atmospheric research.

2.2 Wind Power Density

To compute wind speed and wind power density at different heights, we draw from similarity theory in boundary layer dynamics. Similarity theory (e.g., Stull, 1988) describes the wind profile in the surface layer. Wind speed, $V(z)$, a function of height, z , above the ground, is explained by surface stress, which is represented by the friction velocity, u_* , and the aerodynamic roughness length, z_0 . The aerodynamic roughness length, z_0 , is defined as the height where the wind speed becomes zero. The friction velocity, u_* , is defined as follows:

$$u_* = \left((u'w')^2 + (v'w')^2 \right)^{1/2} \quad (1)$$

where u , v , and w stand respectively for eastward, northward, and vertical surface wind components, and $u'w'$ and $v'w'$ respectively stand for kinematic flux of u and v momentum in the vertical.

Moreover, over land, if the individual roughness elements are packed very closely together, then the top of those elements begins to act like a displaced surface. It can be defined as a displacement distance, d , and a roughness length, z_0 , such as:

$$V(z) = \left(\frac{u_*}{k} \right) \log \left(\frac{z-d}{z_0} \right) \quad (2)$$

for statically neutral conditions, where $V(z)$ is defined to be zero at $z = d + z_0$. An additional term, Ψ , is employed to describe the effects of stability in the boundary layer on $V(z)$ and can thus be expressed as:

$$V(z) = \left(\frac{u_*}{k} \right) \log \left(\frac{z-d}{z_0} - \Psi \right) \quad (3)$$

For this study, the boundary layer is assumed to be neutrally stable, avoiding thus the consideration of Ψ . This assumption seems reasonable knowing that, at the high wind speeds at which wind power is harvested, the boundary layer has large wind shear making it approximately neutrally stable (Stull, 1988). As a result, only Equation 2 is used to compute wind speed at different heights.

During the 1990s the wind turbine hub-height was typically installed at 50 m. With the advancement of technology, the hub height of the turbine has been raised to 80 m, 100 m and 120 m. (Turbines of 80 m hub-heights are most common now.) Thus, the estimation of wind resource and its variability at these different heights is imperative when studying the behavior of wind power over Europe. To compute the wind power density at different heights, it is assumed that the air density does not differ appreciably at these heights through the well-mixed boundary layer. Thus, using the air density, ρ , at the center of the lowest model layer and the wind speed computed using the logarithmic wind profile above, the wind power density (WPD) at these heights is estimated with the following equation:

$$\text{WPD} = \frac{1}{2} \rho V(z)^3 \quad (4)$$

One of the most salient aspects in renewable energy studies—in particular for wind and solar energies—is the variation of these energy resources over time and space. Given the large variability in generated power that can occur within a single day or even a single hour, the connection of an intermittent energy source to the grid requires accurate and informed management to prevent system failures. This is a growing concern as renewable, intermittent energy resource shares increase among the member states' energy mixes. For example, Cox (2009) found that the intermittent nature of wind power makes the power prices very volatile in

British and Irish electricity markets. When wind generation is high, market prices are slightly depressed, but there are sharp jumps when high or low wind persists. In some cases, when wind is very high, prices can even be negative. Lund (2005) reiterates the fact that wind's intermittency limits its applicability as a power source and affects the temporal stability of the frequency and voltage of power generation, thus altering the quality of power. Integration of large amounts of intermittent wind power results in reduced conventional generation, much as thermal and hydropower plants efficiency decreases when operated below their optimum capacity. On a longer time scale, the variability of wind power affects the adequacy of power capacity.

To quantify this variation, previous studies (e.g., Holttinen, 2005; Holttinen et al., 2008; Estanqueiro, 2008) used standard deviation. As a normalized measure of dispersion of a distribution, the coefficient of variation (CoV) is an easily-understood metric and is employed here to evaluate dispersion of distributions around their mean values. The coefficient of variation is defined as follows:

$$\text{CoV} = \frac{\sigma}{\mu} \quad (5)$$

with μ the mean of the variable computed and σ the standard deviation defined by:

$$\sigma = \left[\frac{1}{n-1} \sum_{i=1}^n (x_i - x)^2 \right]^{1/2} \quad (6)$$

where $x = \frac{1}{n} \sum_{i=1}^n x_i$ and n is the number of elements in the sample. Mean and standard deviation are computed in time, and $n = 271,752$ corresponds of the number of hours between 12:30 A.M. January 1, 1979 and 11:30 P.M. December 31, 2009, for the length of our data set.

3. CHARACTERIZATION OF WIND POWER RESOURCE

3.1 Descriptive Statistics of Wind Power

3.1.1 Mean and Median WPD

Figures 1 and 2 show respectively the mean and median WPD at 80 m hub height. The areas left blank denote the areas where the mean or median WPD is below the 200 Wm^{-2} . The choice of this threshold value is based on previous work by Gustavson (1979) and Elliot et al. (1987), and denotes a value of WPD below which no usable wind power is considered to be harvestable with larger capacity (i.e. $>1.5 \text{ MW}$) turbines. What is striking at first is the existence of an onshore "Aeolus crescent", spanning from northern France to Ukraine, of mean WPD ranging from 200 to 350 Wm^{-2} that is absent in the median WPD. Generally speaking, the median values are almost half to the mean value. More specifically, this means that, through the Aeolus crescent

pattern of mean WPD seen in Figure 1, strong but infrequent winds occur such that more than 50% of the time the WPD value is quite lower than its mean. The areas that show higher WPD values are those located on the English Channel, North Sea and Baltic Sea mainland shores as well as the British, Irish, Danish, Icelandic and Scandinavian shores on the Atlantic Ocean side. This is consistent with present wind turbine deployment, except for Spain, for instance, which ranks second in term of installed capacity in 2011 (Wilkes et al. 2012).

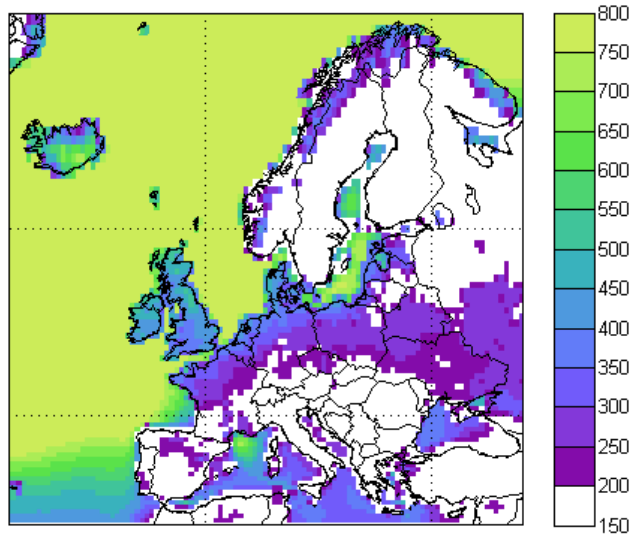


Figure 1. Geographical variation of the mean wind power density at 80 m. computed with MERRA data.

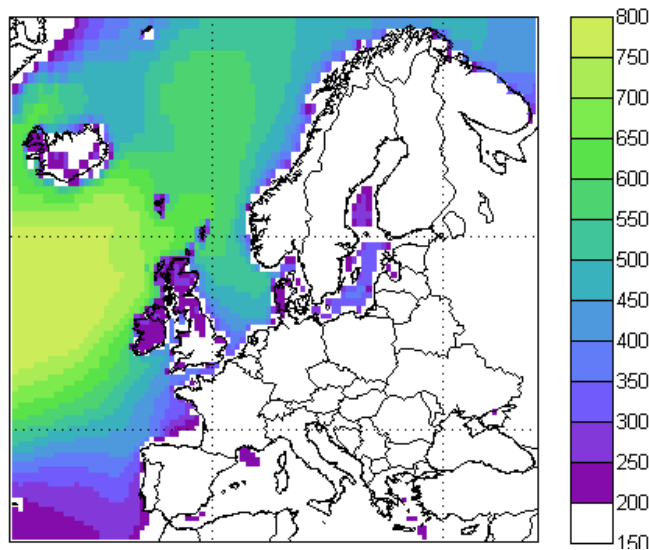


Figure 2. Geographical variation of the median wind power density at 80 m height over Europe, computed from MERRA data.

3.1.2 Coefficient of Variation of Wind Power

For two regions with the same mean WPD, the one with a lower standard deviation (and thus lower CoV) is preferable since the power generated is less variable. Similarly, for two regions with the same standard deviation, the one with greater mean WPD is preferable and this one will have a lower CoV. Given the impact of variability in wind power on the electric grid, and the economics of power generation and distribution, emphasized by Cox (2009) for instance, it is more favorable to deploy wind turbines in regions of low CoV. To assess this strategic deployment consideration, **Figure 3** presents the CoV of wind power density at 80 m hub height. The CoV is especially low (values ranging from 1.2 to 1.4) across Portugal, central-southern France, the United Kingdom, Ireland, most of Lithuania and Belarus as well as northern Russia, southern Finland, Sweden and southern Norway.

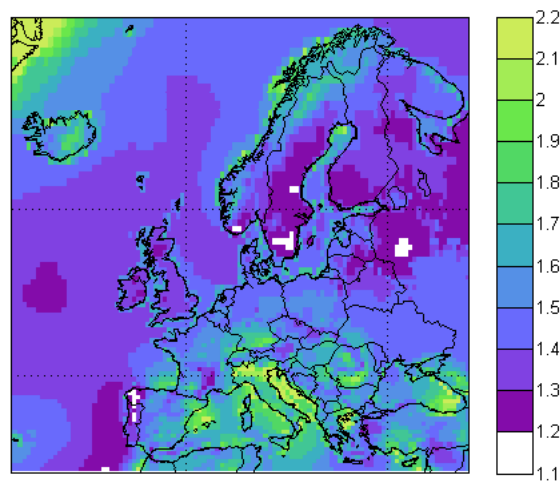


Figure 3. Geographical variation of the coefficient of variation (dimensionless) of the wind power density at 80 m, computed from MERRA data.

3.1.3 Interquartile Range

The Interquartile Range (IQR) is a robust estimate of statistical dispersion. Here it signifies the difference between the 75th and the 25th percentiles of the WPD time series at each location, as displayed on the **Figure 4**. When there are outliers in the data, which is especially true for the long-tailed wind distributions as seen in this study, the IQR is said to be more representative than the standard deviation and CoV as an estimate of the spread of the body of the time series considered. The IQR represents the possible “swings” of the WPD at a location.

Continental Europe, southern countries and Scandinavian Peninsula show low IQR—below 200 Wm^{-2} . Coastal countries, from western France to Estonia, display greater values, ranging from 300 to 600 Wm^{-2} . The maximal inland IQR values, up to 1000 Wm^{-2} can be found in the United Kingdom, Ireland and Iceland. The far offshore Atlantic also has very large IQR—above 1400 Wm^{-2} .

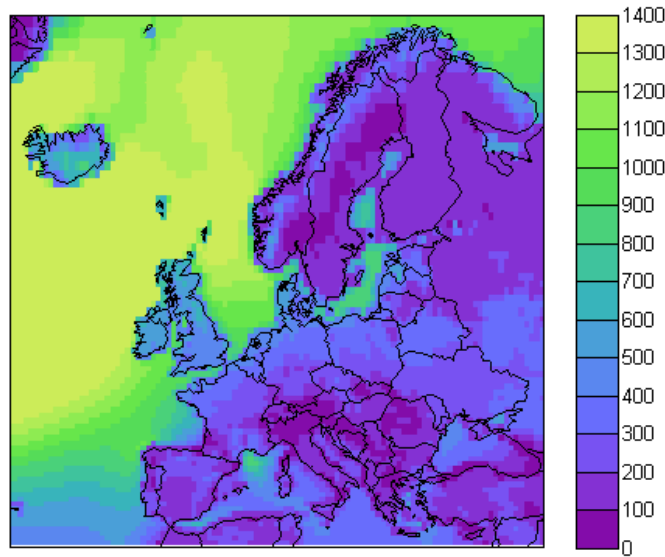


Figure 4. Geographical variation of the interquartile range of wind power density at 80 m over Europe, computed from MERRA data.

4. WIND DATA ASSESSMENT AND COMPARISON WITH PREVIOUS STUDIES

4.1 Comparison with Archer (2005)

We consider the results from Archer (2005) in which wind speed and temperature data from NCDC (National Climatic Data Center) and FSL (Forecast Systems Laboratory) for the years 1998–2002 are employed. The raw data comes from thousands of surface stations and from hundreds of sounding stations around the world and provides daily averaged wind speed measurements at a standard elevation of 10 m above the ground. In some cases, these surface stations also provided hourly measurements at an elevation of 80 ± 20 m above the ground. To obtain estimates of wind speed at 80 m at all sites, a revised Least Square methodology is introduced and its performance is assessed through the comparison between the data computed and observational data from 23 towers around the Kennedy Space Center. It should be noted that statistics in the Archer study were applied only to the year 2000 in order to be compared with previously published work.

Both **Figures 5 and 6** show that the greatest potential in Europe is located along the northeastern coasts, particularly in France, Belgium, Netherlands, Germany, and Denmark. The coasts of the United Kingdom and the islands in the North Sea present high wind speed as well. Overall, the coastal patterns and locations of the relative minimum and maximum between the Archer and MERRA results are qualitatively consistent, even if absolute values differ. The results from Archer (2005) appear characteristically higher than the MERRA mean wind speeds. For inland mean wind speeds, the results from MERRA are qualitatively consistent with results from Archer (2005), mainly below 6.9 m/s. It should be borne in mind that as Archer (2005) displayed results for one year (2000) as well as for discrete locations (not gridded as in MERRA); thus this comparison only aims at qualitative remarks.

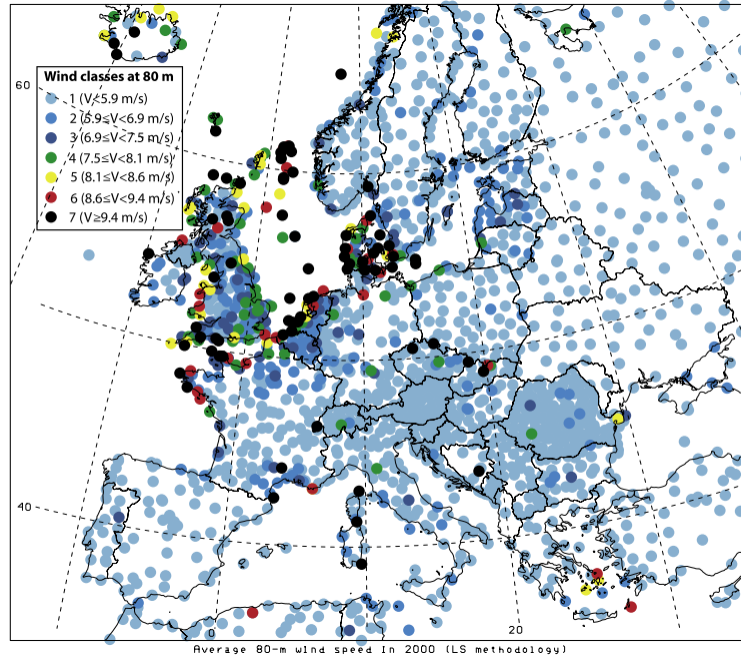


Figure 5. Map of wind speeds (m/s) extrapolated to 80 m and averaged over all days of the year 2000 at surface and sounding stations with 20 or more valid readings in Europe, from Archer (2005).

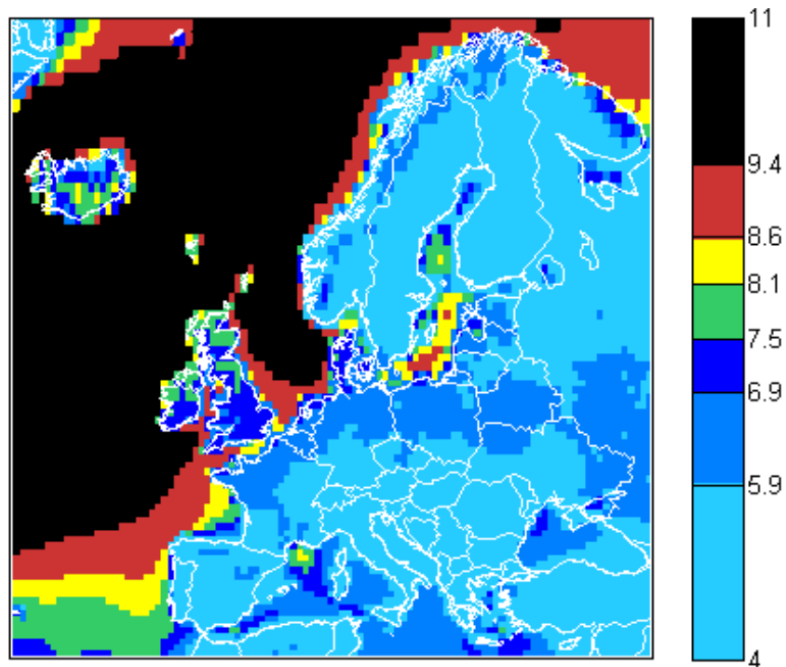


Figure 6. Geographical variation of the mean wind speed at 80 m height over Europe, computed from MERRA data and using the same color scale as Archer (2005).

4.2 Comparison with EEA Report

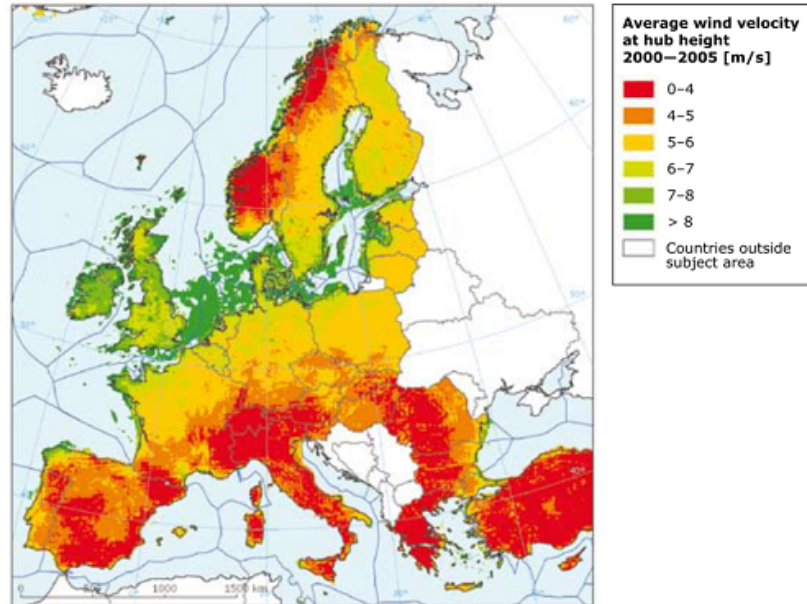
The European Environmental Agency (EEA) study (EEA, 2009) uses the ECMWF 44-year reanalysis data at 10 m height as the primary resource. Average wind speeds for the period

2000–2005 were used to generate the map displayed here. The wind speeds used in the computations were derived from the 10 m height wind. The meteorological gridded data for the years 2000–2005 were transformed into the grid format used by ESRI (a firm specializing in geographic information software). Both the original six-hour and the daily/monthly meteorological parameter values were converted into annual averages at the given grid resolution. As explained in EEA (2009), ESRI's six-hour values were averaged to half-month values and daily values were averaged to two-month values. These intermediate average values were in turn used to derive annual averages. The 10 m wind speed values derived were subsequently recalculated to correspond to wind turbine hub heights of 80 m onshore and 120 m offshore. To derive the wind velocity at hub height—assumed to be 80 m onshore and 120 m offshore—the following formula was used:

$$V_H = V_{10} \left[\frac{\ln\left(\frac{H}{z_0}\right)}{\ln\left(\frac{10}{z_0}\right)} \right] \quad (7)$$

where H stands for the hub height expressed in m, V_H is the wind speed at hub height expressed in m/s, V_{10} is the wind speed at 10 m height expressed in m/s and z_0 is the roughness length expressed in m.

For the EEA average wind velocity map shown in **Figure 7**, it must be emphasized that “hub height” refers to 80 m from the surface for onshore and 120 m for offshore winds. Thus, when comparing results with MERRA, we consider the corresponding 80 m (**Figure 8**) for onshore and 120 m (**Figure 9**) for offshore wind maps. Qualitatively, the relative wind patterns from the MERRA results look quite consistent with EEA results, which is encouraging for the assessment of the relevance of MERRA data over Europe. Taking a closer look, onshore wind speeds computed with MERRA tend to be lower near the coast, especially the English Channel coasts and North Sea coasts. Further inland, lower mean wind speeds are seen across Central Europe for MERRA compared to the EEA estimates. As for offshore mean wind speed, although limited in areal extent, the EEA values generally agree with MERRA.



Source: EEA, 2008.

Figure 7. Average wind velocity at hub height (80 m onshore and 120m offshore) 2000-2005 (EEA, 2009).

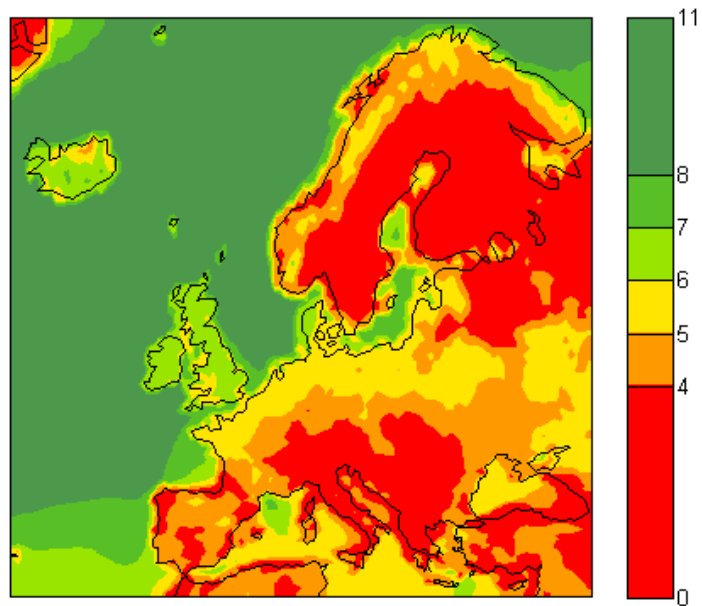


Figure 8. Geographical variation of the mean wind speed at 80 m height, computed from MERRA data and using the same color scale as EEA (2009).

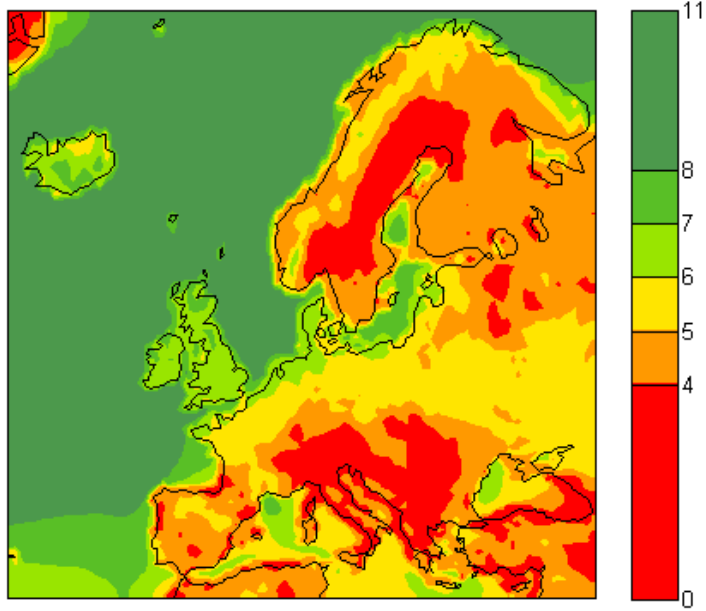


Figure 9. Geographical variation of the mean wind speed at 120 m height over Europe, computed from MERRA data and using the same color scale as EEA (2009).

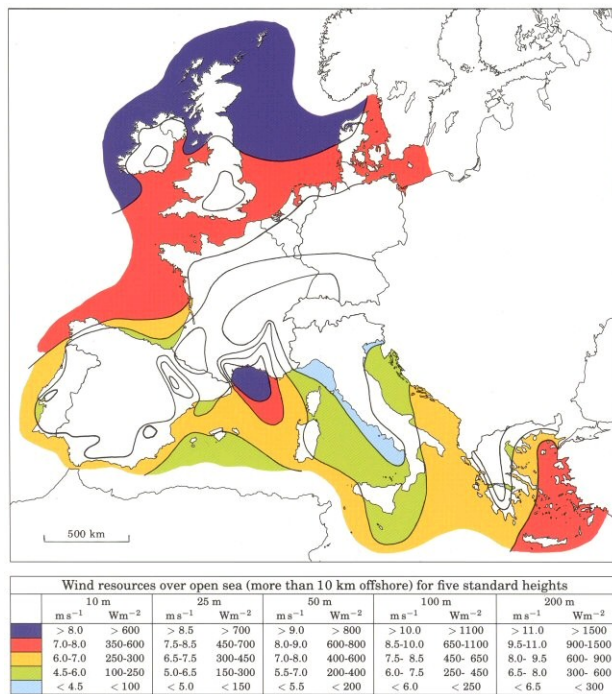
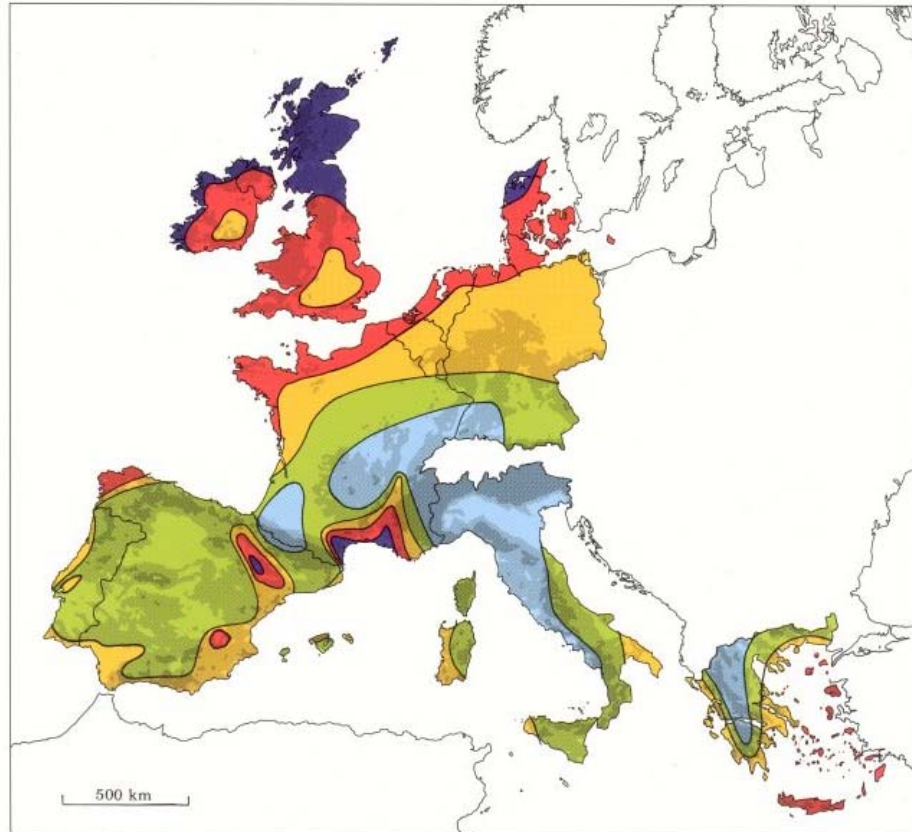


Figure 10. Offshore mean wind speed and wind power density computed by the Risø National Laboratory for five standard heights (10, 25, 50, 100 and 200 m).

4.3 Comparison with Risø National Laboratory Assessment

The data used by the Risø National Laboratory in Troen and Petersen (1989) comes from more than 200 meteorological stations all over EU-12 (Belgium, Greece, Luxembourg, Denmark, Spain, Netherlands, Germany, France, Portugal, Ireland, Italy, and the United Kingdom) and usually cover ten years of measurements. For offshore data, there are very few stations considered in the study, and the wind speed and wind power density estimates are quite uncertain.

Variations of wind speed obtained from MERRA data differ sharply between the onshore and offshore results (**Figures 10 and 11**, respectively) from Troen and Petersen (1989). As for wind power density, the contrast between Figure 11 and **Figure 12**, at 50 m height, is less striking than for the comparison of wind speeds at 100 m, on **Figure 13**. This comparison reveals several distinctions between the data sets, with the largest contrasts occurring over inland areas. As noted by Troen and Petersen (1989), “in the Mediterranean some regions enjoy—from a wind energy point of view—the benefits of certain particular atmospheric processes giving rise to favorable wind conditions. Well-known wind systems are the Mistral, the Tramontana and the Bora”. It may be useful to bear in mind that the Mistral is a strong wind in France, coming from the north or northwest and which accelerates when it passes through the valleys of the Rhône and the Durance Rivers toward the coast of the Mediterranean around the Camargue region. The Tramontana is similar to the Mistral in its causes and effects, but it follows a different corridor; it accelerates as it passes between the Pyrenees and the Massif Central, and the Bora is a northern to north-eastern katabatic wind in the Adriatic, Bosnia and Herzegovina, Croatia, Montenegro, Italy, Greece, Slovenia, and Turkey. While MERRA is able to account for varying land types though the displacement height and roughness length, additional aspects specific to mountainous regions may not be adequately resolved, and are likely a cause for the lower estimates over southern France along the Mediterranean coast.



Wind resources ¹ at 50 metres above ground level for five different topographic conditions										
	Sheltered terrain ²		Open plain ³		At a sea coast ⁴		Open sea ⁵		Hills and ridges ⁶	
	m s ⁻¹	Wm ⁻²	m s ⁻¹	Wm ⁻²	m s ⁻¹	Wm ⁻²	m s ⁻¹	Wm ⁻²	m s ⁻¹	Wm ⁻²
Dark Blue	> 6.0	> 250	> 7.5	> 500	> 8.5	> 700	> 9.0	> 800	> 11.5	> 1800
Red	5.0-6.0	150-250	6.5-7.5	300-500	7.0-8.5	400-700	8.0-9.0	600-800	10.0-11.5	1200-1800
Orange	4.5-5.0	100-150	5.5-6.5	200-300	6.0-7.0	250-400	7.0-8.0	400-600	8.5-10.0	700-1200
Green	3.5-4.5	50-100	4.5-5.5	100-200	5.0-6.0	150-250	5.5-7.0	200-400	7.0- 8.5	400- 700
Blue	< 3.5	< 50	< 4.5	< 100	< 5.0	< 150	< 5.5	< 200	< 7.0	< 400

From the *European Wind Atlas*. Copyright © 1989 by Risø National Laboratory, Roskilde, Denmark.

Figure 11. Onshore mean wind speed and wind power density at 50 m above ground level for five different topographic conditions (sheltered terrain [urban districts, forest and farm land with many windbreaks], open plain [open landscapes with few windbreaks], at a sea coast, open sea [more than 10 km offshore], hills and ridges [correspond to 50% overspeeding and calculated for a site on the summit of a single axisymmetric hill with a height of 400 m and a base diameter of 4 km]), computed by the Risø National Laboratory.

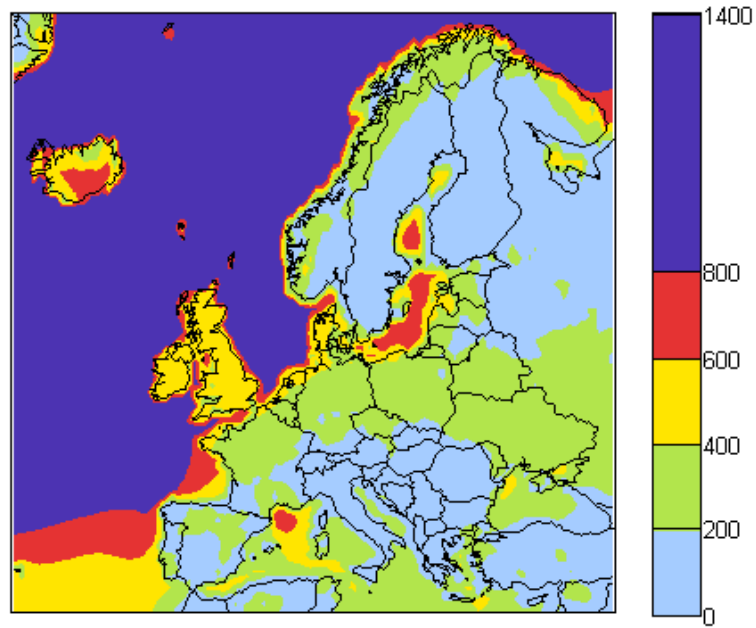


Figure 12. Geographical variation of the mean wind power density at 50 m over Europe, computed from MERRA data and using the same color scale as Troen and Petersen (1989).

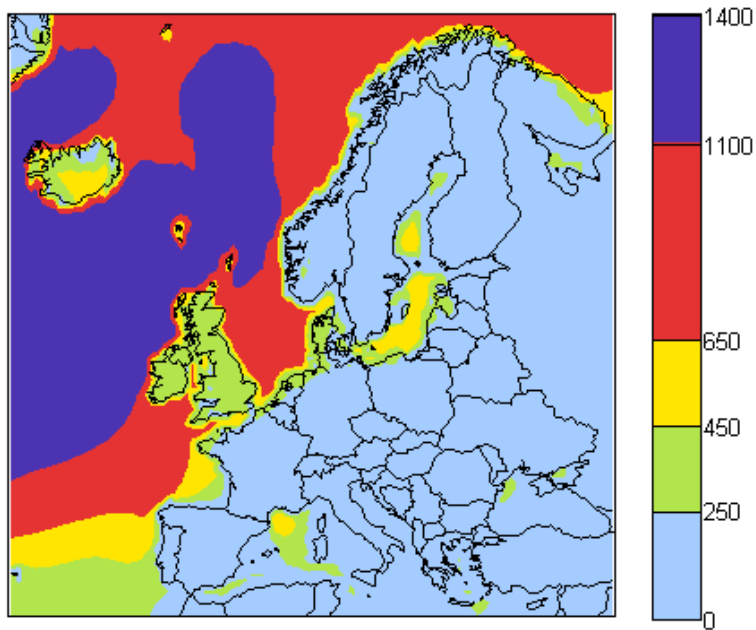


Figure 13. Geographical variation of the mean wind power density at 100 m over Europe, computed from MERRA data and using the same color scale as in Troen and Petersen (1989).

5. FURTHER ASSESSMENT OF THE WIND POWER RESOURCE

5.1 Availability of Wind Power

To further assess the wind power resource, its availability is considered. This is a way to test the reliability of a system. Extending the concept to wind power, the availability of wind power at a location has been estimated as:

$$Availability = \frac{\# \text{ of hours with } WPD \geq 200 \text{ Wm}^{-2}}{\text{Total \# of hours}} \quad (8)$$

Figure 14 shows the availability of wind power over Europe. The greatest availability onshore is found in Ireland, the United Kingdom, Denmark, and on the English Channel, North Sea and Baltic Sea coasts. Surprisingly, the availability in the Alps is very low, even though it might seem that mountains would have high wind power resources. This could be due to the decrease in air density as altitude increases, but it may also be partly attributed to difficulties in MERRA resolving these mountainous regions.

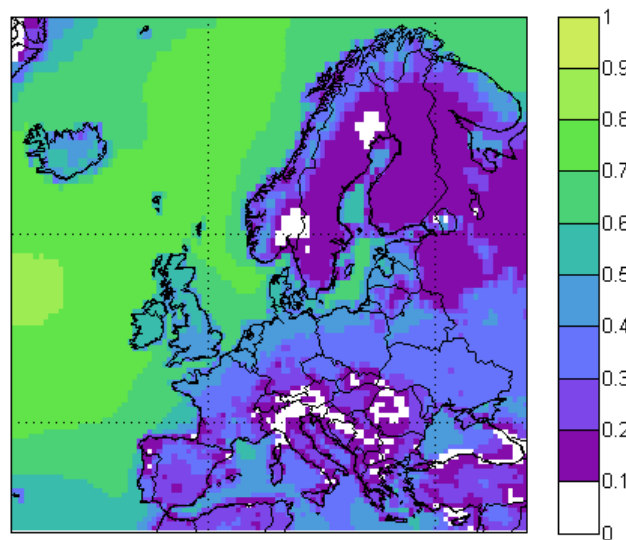


Figure 14. Geographical variation of dimensionless availability of wind density power at 80 m over Europe, computed from MERRA data.

5.2 Capacity Factor Analysis

The availability presented above can be considered as an upper bound of the capacity factor, CF, which is defined as the fraction of the rated power—or maximum capacity—produced in a year. Given the exceptional length of the database used here, this definition is extended to be the rated power produced on an hourly basis over 31 years, from 1979 to 2009. A study about the power harvested implies the choice of a referenced wind turbine to undergo capacity factor

computations. According Vestas (2012a and 2012b), the Vestas wind turbine suits all the ranges of wind-classes and is produced in onshore and offshore versions.

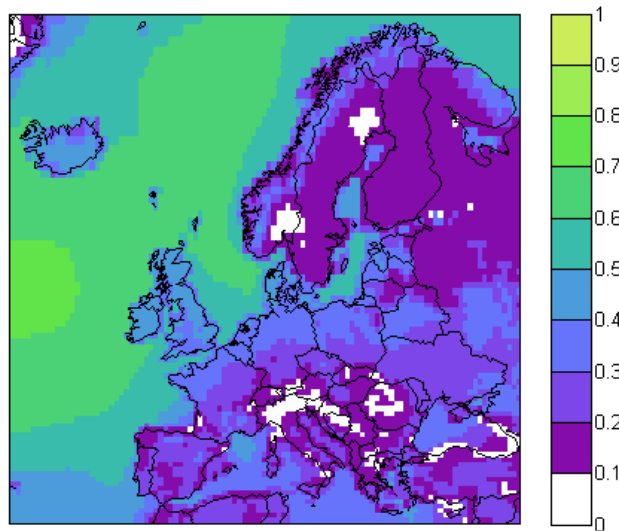


Figure 15. Geographical variation of the mean capacity factor at 80 m over Europe, computed from MERRA data.

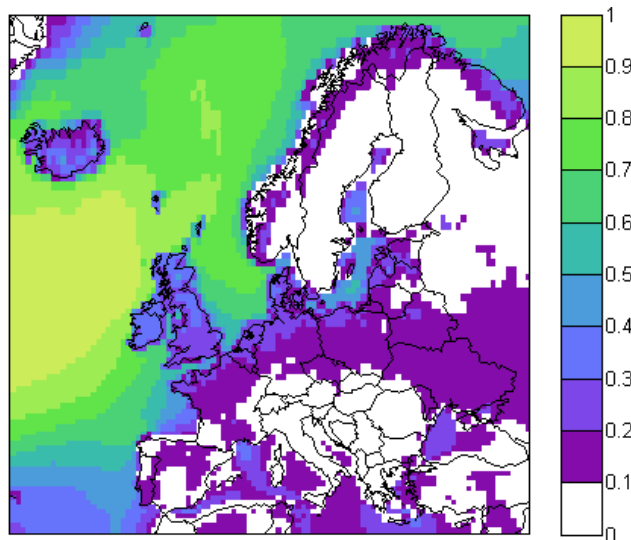


Figure 16. Geographical variation of the median capacity factor at 80 m over Europe, computed from MERRA data.

Figure 15 and 16 are display the mean and median results over the thirty-one years of the database. The wind speed used to compute this CF is the wind speed at 80 m height, since the hub height of the Vestas wind turbine used is 84 meters. The results are consistent with the availability of the wind power density at 80 m, displayed on Figure 14. According to the results displayed on Figure 15, Iceland, Ireland, the United Kingdom, and Denmark have the highest onshore capacity factor mean values, from 0.4 to 0.5. The second best onshore areas are the

Aeolus crescent noted earlier (that spreads from northwestern France to western Ukraine) and over the Kjolen Mountains with mean values ranging from 0.2 to 0.4. As for offshore regions, the best accessible spots remain along the Atlantic coasts, from western France to Estonia with mean values up to 0.6. The potential over the Mediterranean and the Black Sea is lower with its maximal mean values up to, respectively, 0.5 and 0.4.

The behavior of the median values (Figure 16) compared to the mean values is, at first, surprising. For example, while inland, the Mediterranean and Black seas' median values are approximately equal to half of the mean values, while Atlantic offshore median values increase compared to mean values. This difference in the relationship of median to mean can be explained by the different behaviors of onshore versus offshore winds. Offshore winds blow more regularly and with higher intensity than onshore winds due to low roughness over the open ocean.

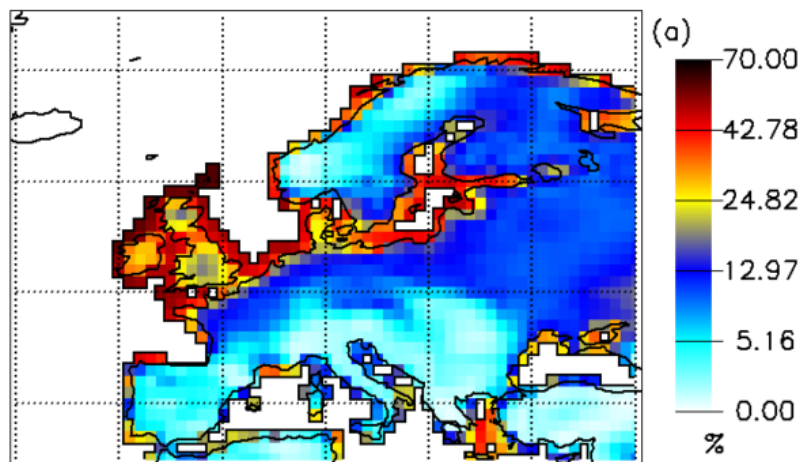


Figure 17. Average wind power in unit of percentage capacity factor, from Kiss and Janosi (2008).

To qualitatively compare these results with previous work, the study from Kiss and Janosi (2008) can be considered (**Figure 17**). They used the ERA-40 data bank covering a period of 44 years with a temporal resolution of 6 hours. Instantaneous wind speed values are provided in geographic cells of size $1^\circ \times 1^\circ$ for 10 m and 1000 hPa pressure heights. As previously mentioned, the time and spatial resolution of the MERRA data is hourly and grid cells of $1/2^\circ \times 2/3^\circ$. Other differences lie in the processing. Since they worked with raw-data wind speeds at 10 m height, they extrapolated to hub heights they considered, from 60 m to 120 m height. In doing so, they “introduced the simplest possible estimate based on the available data which is the multiplication of instantaneous wind speeds at 10 m by a factor of 1.28”. They are thus not taking into account geographical variation in friction velocity, roughness length and displacement height as done here. This may explain many of the differences seen. For central Europe and Spain, relative variations are consistent but absolute values are higher in this study. However, they emphasized that, “the simple method [they] implemented for wind speed estimates at higher elevations can be a source of numerical errors”. Nevertheless, there is a qualitatively good match between these estimates over Ireland, the United Kingdom and the

offshore regions considered in the study. Scandinavian Peninsula shows a dissatisfactory comparison and may result from the inadequate representation of the Kjolen Mountains.

5.3 Distinction between Variability and Intermittency

In previous studies, intermittency is used to characterize the availability of wind. Here, both intermittency and variability are considered. Intermittency will refer to the switch between power generation and no power generation states. If the wind power density falls below the threshold of 200 Wm^{-2} , it is assumed that no power can be generated, which means that a turbine placed in the area would presumably produce no usable power. Conversely, if the wind power density is above this value and if there are wind turbines at the considered location, wind energy is harvestable over time. Variability will refer to variations of wind power intensity when wind power is at least sufficient to be usable and thus is used to describe changes over time in the generated power.

Figure 18 illustrates the distinction explained in the previous paragraph. It shows wind power density at a location in the central U.S. for 200 consecutive hours. The red horizontal line represents the threshold of 200 Wm^{-2} . For the first 21 hours, the wind power density is above this minimum, but it varies. This variation is what we will distinguish as variability. For some of the time, for instance from 140th hour to 200th hour, the wind power switches from values below the 200 Wm^{-2} threshold to values above it; this is what it is characterized as intermittency.



Figure 18. Illustrative wind power density profile showing fluctuations in wind, from Gunturu and Schlosser (2011).

5.4 Wind Episodes Lengths

This analysis not only focuses on characterizing the extent of wind power resource, but also its intermittent and variable behavior, quantified first by wind episode length (WEL). This

measure corresponds to the number of consecutive hours during which the WPD is above 200 Wm^{-2} . It measures the persistence of wind power and can therefore serve as an indicator for the reliability of power generation.

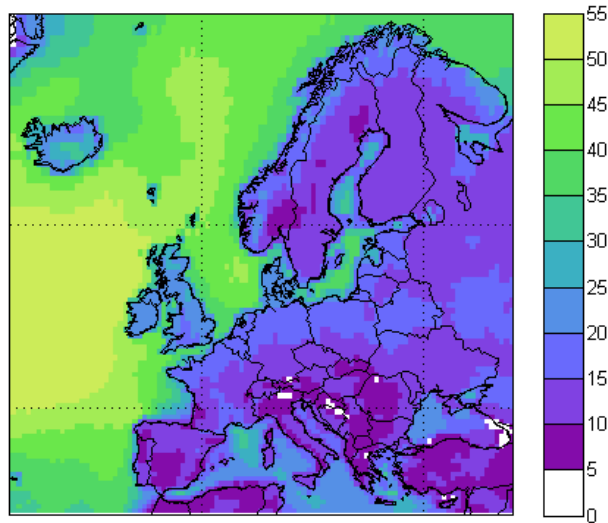


Figure 19. Geographical variation of the mean wind episode length (hours) at 80 m, computed from MERRA data.

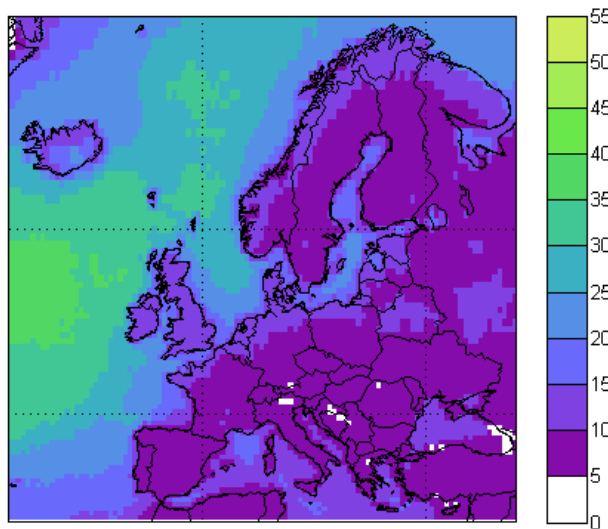


Figure 20. Geographical variation of the median wind episode length (hours) at 80 m, computed from MERRA data.

Episode lengths were computed directly from the MERRA data, as explained in Gunturu and Schlosser (2012). The geographical distribution of the mean wind episode length at 80 m (**Figure 19**) shows a wide range from 5 to 55 hours. Southern Europe as well as Sweden, Finland and northwestern Russia display the lowest WELs, below 15 hours. Meanwhile, WELs in coastal countries, from northern France to Estonia, the United Kingdom, Ireland, the Atlantic side of Norway and Iceland are higher, at up to 30 hours. The maximum WELs (above 55 hours) are reached in far offshore areas. Overall, offshore winds tend to be stronger and steadier than onshore winds, due to reduced roughness above oceans. However, in the Mediterranean and the Baltic Sea, the WEL behaves more like onshore winds than offshore ones. Finally, as noted for the mean and median WPD, the median WEL (**Figure 20**) is approximately half of the mean value.

5.5 Spatial Coincidence of Intermittency

The geographical correlation of wind episodes across Europe has been studied to further analyze intermittency and variability of the wind power resource. To effectively mitigate intermittency through aggregating geophysically dispersed wind turbines, wind must be present at at least one of two (or more) connected sites. The extent of this condition is quantified using the construct described below, with the goal of assessing the potential benefit of integrated wind farms. Each and every grid point has been considered as well as its nine closest neighbor grid points in each direction (drawing thus a 19×19 grid-box domain—approximately $1000 \text{ km} \times 1000 \text{ km}$ centered about the grid point of interest) to determine if they had wind when the considered point had or had not. For these grid points, time series of wind and no-wind states are compared between the grid point considered with respect to its surrounding points in the $1,000 \text{ km}^2$ domain. **Figure 21** illustrates the process. The center of a box is R, and another point P is chosen. Then the covariation of the wind resource state at these two points is studied. The number of points in the box around R that fulfill the anticoincident WPD criterion is the score of the point R. To determine the anticoincident WPD criterion, the hours when there is wind state—WPD greater than 200 Wm^{-2} —at one of the two points (P and R) but not both, are counted. If this count is at least 50% of the total length of the time series, the two points are said to be “anticoincident”—and the criterion is fulfilled. As explained in details in Cosserson et al. (2013) and based on a methodology first developed by Gunturu and Schlosser (2011), two specific variables—antiCoincidence and antiNullCoincidence parameters - have been built. The first one "anticoincidence" corresponds exactly to the description of the criterion above. The second metric, "antiNullCoincidence", considers only situations when the central grid point has no usable WPD and determines the number of surrounding grids (within the 19×19 grid) that have usable WPD for at least 50% of these situations.

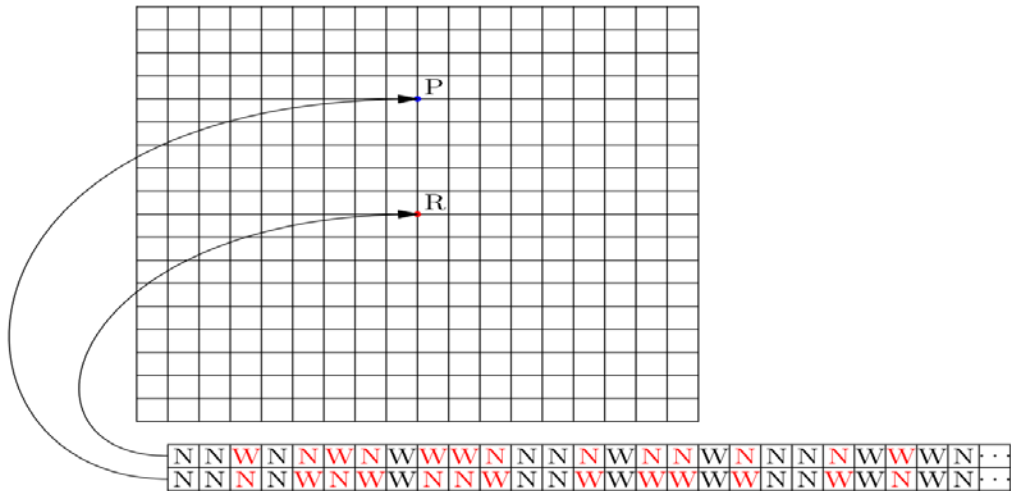


Figure 21. Sketch illustrating the criterion for antiCoincidence, from Gunturu and Schlosser (2011).

5.5.1 AntiCoincidence

Figure 22 shows the geographical variation of normalized antiCoincidence of WPD at 80 m height over Europe. The color of each grid point shows the number of anticoincident points in a box of approximately 1000 km × 1000 km around it, divided by the total number of points in the box. The white region shows complete lack of antiCoincidence and thus, complete coincidence of intermittency. Points that have greater concentration of anticoincident points around them would presumably benefit more strongly from interconnection. Only the center of the Scandinavian Peninsula, northwestern Spain, and northern Portugal show a significant fraction of anticoincident points. These values remain quite low for Scandinavian Peninsula, in contrast to Spain and Portugal, where for some points nearly half of the grid points in a region of approximately 1000 km × 1000 km are anticoincident.

To understand this large coincidence in intermittency, we consider the topographic and climate features of Europe (**Figures 23 and 24**). In contrast to the United States case conducted by Gunturu and Schlosser (2011), the large lack of antiCoincidence cannot be explained here by uniform low surface roughness linked to semiarid climate and even terrain. As illustrated in Figures 23 and 24, mountainous areas cover the region of very low antiCoincidence, mainly the Spanish Meseta, the Pyrenees, the Alps, the Balkan Dinaric Alps, and the Kjolen Mountains. Even if the altitudes reached are about the same elevation as the North American Rockies, they occupy areas too limited to significantly impact winds at the continental scale.

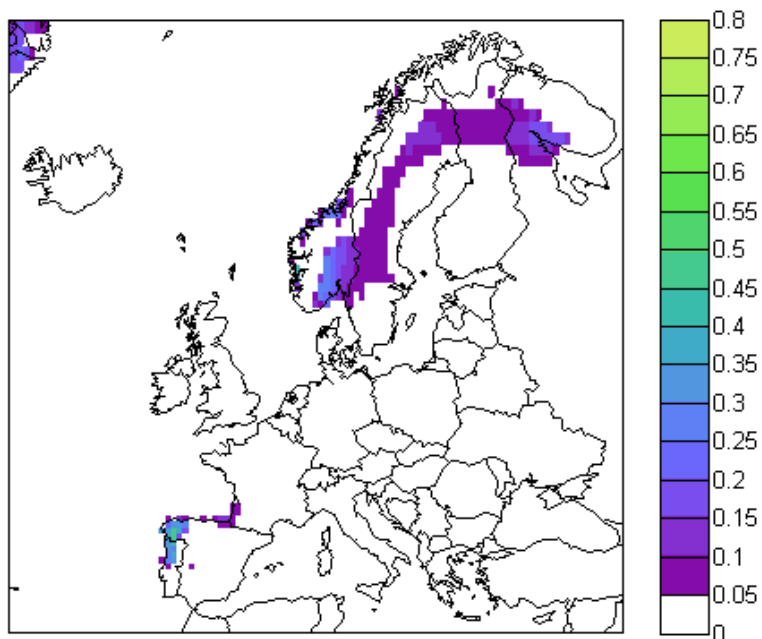


Figure 22. Geographical variation of the normalized antiCoincidence parameter at 80 m over Europe, computed from MERRA data.



Figure 23. Topographic map of Europe (from <http://www.worldatlas.com/>).

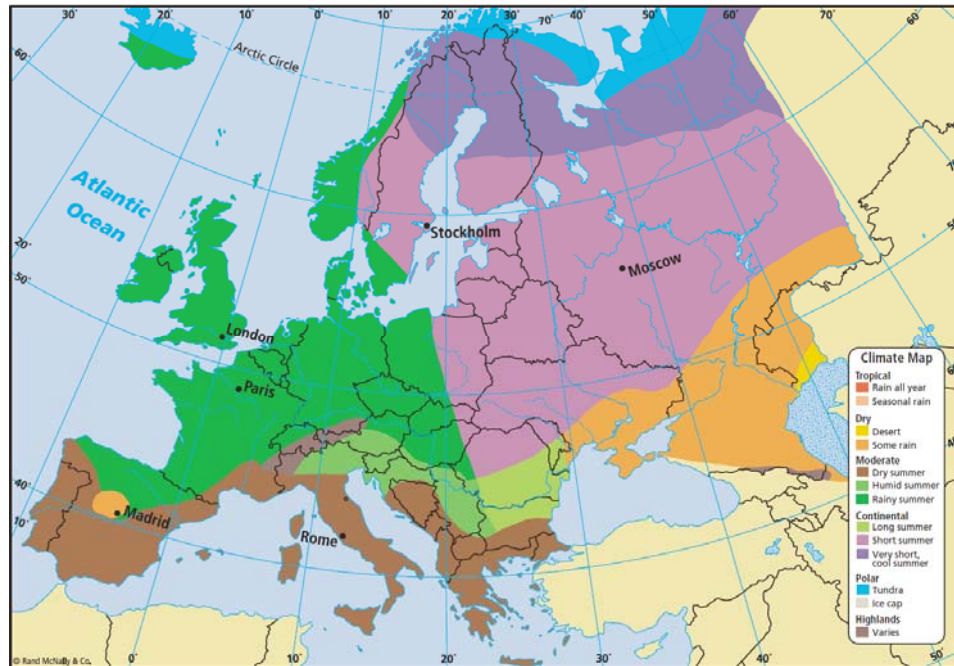


Figure 24. Climate map of Europe (from <http://education.randmcnally.com/>).

5.5.3 AntiNullCoincidence

The geographical variation of normalized antiNullCoincidence of WPD at 80 m height over Europe is shown in **Figure 25**. The white regions show complete lack of antiNullCoincidence. Significant antiNullCoincidence is found for Iceland, Norway, Scotland, Ireland, and Northwestern Spain where the antiNullCoincidence values reach as high as 0.7 and 0.8. This means that, if there is no sufficient wind at one of these points, there are many sites around the point that have sufficient wind, and interconnecting these sites can provide a steadier wind power supply. It can be noted that in the case of antiCoincidence, offshore regions do not have sufficient antiCoincidence, and are more likely to show antiNullCoincidence. The most significant lack of antiNullCoincidence occurs in the eastern and southeastern parts of Europe. Apart from the ramifications of this result for interconnecting mitigate intermittency, this is significant in that the intermittency in the eastern and southeastern parts of Europe are highly synchronized due to high coincidence. Thus, interconnecting these regions could pose a challenge for the electric grid; synchronized high wind situations will deliver a large amount of wind power to the grid, and synchronized low wind situations will result in low wind power output. Therefore, storage and/or backup generation technologies would be required to provide a more reliable power production from large wind-farm deployment.

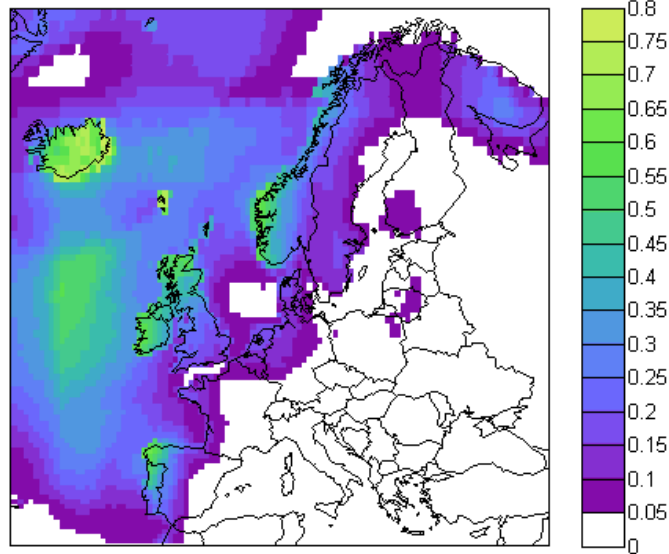


Figure 25. Geographical variation of the normalized antiNullCoincidence parameter at 80 m over Europe, computed from MERRA data.

6. WIND POWER RESOURCE AT DIFFERENT HUB HEIGHTS

6.1 Wind Power Density at Various Hub Heights

During the 1990s the general wind turbine height was 50 m. With the advancement of technology, the hub height of turbines has been raised to 80 m, 100 m and 120 m, although turbines of 80 m hub height are more common now. The cutting-edge turbine considered for the capacity factor analysis (Section 4.2.2) reaches 84 meters height, Vestas (2012a). The wind resource and its variability at these different heights is then estimated to assess the relevance to move toward higher and higher hub heights. The difference between the various heights is displayed in terms of relative change (R_{change}) defined as follows:

$$R_{change} = \frac{(\text{higher hub value}) - (\text{lower hub value})}{(\text{lower hub value})} * 100 \quad (9)$$

The use of R_{change} can be misleading without bearing in mind that it is a relative value. For instance, over the Alps, the relative change is high (above 50%) in each case and this is partly because median WPD values at these locations are extremely low. Thus small absolute changes from very low values lead to high relative variations. Moving from 50 m to 80 m (**Figure 26**) or from 80 m to 120 m (**Figure 28**) is beneficial in terms of WPD reached, especially for northwestern Spain, western Balkans and Northeastern Europe whereas the benefits from moving from 80 m to 100 m are not so obvious (**Figure 27**). The use of relative change is particularly relevant for the analysis of evolution in the coefficient of variation (CoV) between various heights. If there is a slight decrease in the coefficient of variation, it means that the wind power density varies slightly less and thus power generation would be more stable When the coefficient

of variation increases, the relative change is so low, as illustrated **Figure 29**, that the improvement for this particular metric is minimal at higher hub levels.

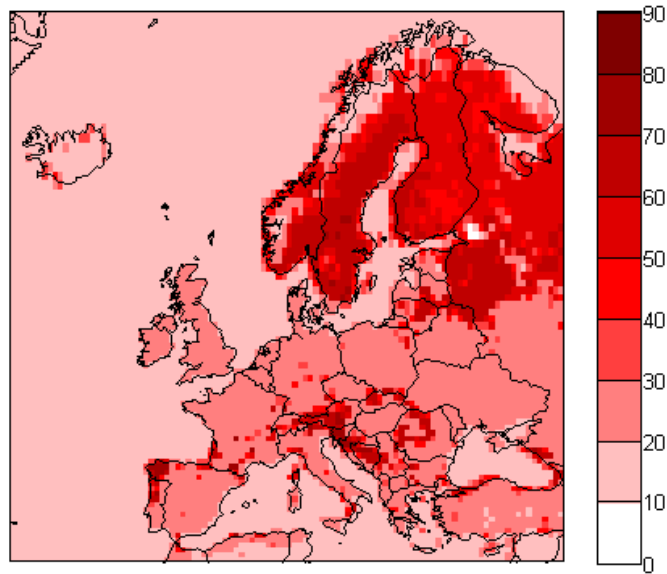


Figure 26. Relative change in the median WPD between 50 m and 80 m height over Europe, computed from MERRA data.

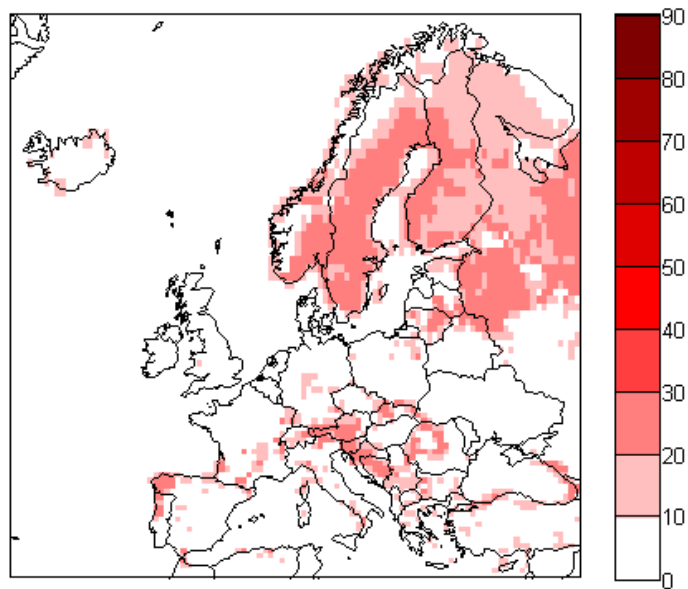


Figure 27. Relative change in the median WPD between 80 m and 100 m height over Europe, computed from MERRA data

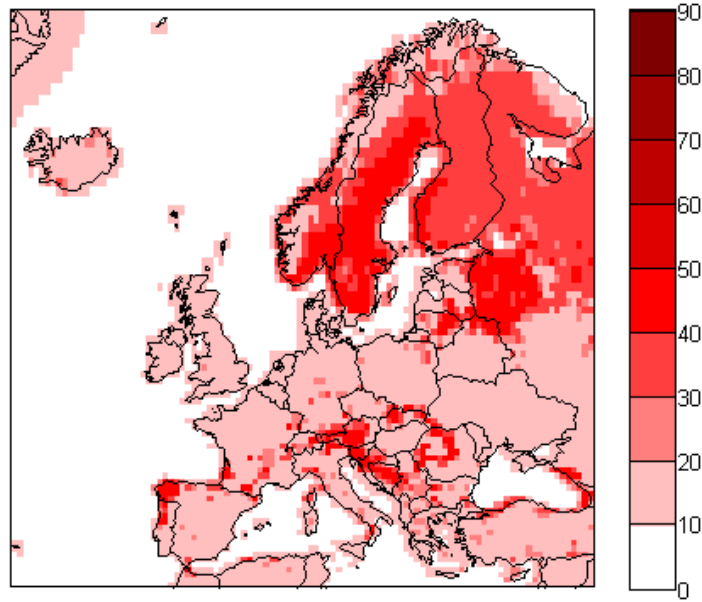


Figure 28. Relative change in the median WPD between 80 m and 120 m height over Europe, computed from MERRA data.

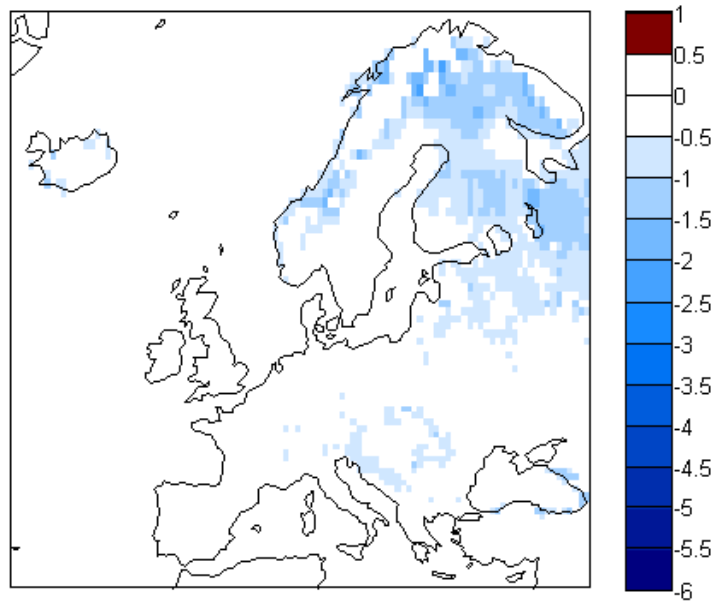


Figure 29. Relative change in the CoV between 80 m and 100m height over Europe, Computed from MERRA data.

6.2 Episode Length at Different Hub Heights

Contrary to the variation shown above, the absolute difference is displayed here, as presented in **Figure 30**, for the variations in median wind power episode length at different heights. The absolute difference is meaningful in regards to episode lengths. As it is quantified in hours, it allows for an assessment of how many hours can be gained by moving hubs higher. Although the

spatial features are quite randomly distributed at small scales, the highest benefits would be for far offshore. Inland benefits are gathered among the Norway, Northwestern Russia, the United Kingdom and Ireland. For the other inland areas, the variations with height seem randomly distributed. To conclude, it appears relevant to raise hubs heights from 80 m to 120 m in term of median WPD reached then. However it may not be a cost-effective project if the goal is to gain in stability, according to the tiny improvements caught with height for CoV and WEL. A more comprehensive understanding of the benefits of higher hub heights would also require consideration of costs and profits.

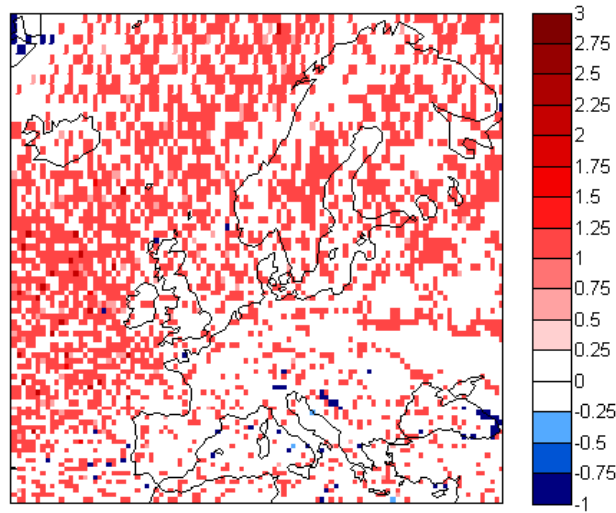


Figure 30. Difference in the median WEL between 80 m and 100 m (h).

7. CONCLUSION

The analyses presented here provide some interesting conclusions. The areas with the “best” wind power sources, defined as being where the wind power density and capacity factor values are high and the coefficient of variation low, are located on the northern coastlines as well as in the United Kingdom, Ireland, and Denmark. In addition, there exists a “second-best” source that spans from northern France to eastern Ukraine and named here as the “Aeolus crescent”. To study the spatial coincidence of intermittency, two parameters—anticoincidence and antiNullCoincidence—were introduced. While only the center of the Scandinavian Peninsula, northwestern Spain and northern Portugal show significant fraction of anticoincident locations, notable antiNullCoincidence is found for Iceland, Norway, Scotland, Ireland and northwestern Spain, which thus would benefit from an interconnection of wind-power installations. Nevertheless, as the occurrence of wind episodes over Europe remains mainly correlated, storage and/or backup generation technologies would be required to provide a reliable power production from large wind-farm deployment. Lastly, it was pointed out that moving wind turbine hub-heights from 50 meters to 80 meters or from 80 meters to 120 meters can be beneficial, especially in northwestern Spain, western Balkans and Northeastern Europe whereas the benefits from moving from 80 meters to 100 meters are not obvious.

Several considerations of this study must be noted. First, the data used for construction of the wind resource is the product of the assimilation of measurements and satellite remote sensing data into a global model. Thus imperfections in the model and the assimilation schemes are bound to influence the computed output. The spatial resolution of the data is $1/2^\circ \times 2/3^\circ$ and thus, some local effects that change wind speeds like mountain passes and valleys are not represented in this study. Furthermore, the time resolution is an hour, and thus only intermittency and other phenomena of timescales longer than an hour and their effects can be studied. Moreover, territorial constraints and social acceptance matters are not considered here. While studying the variation of the wind resource, the demand or load and the economic feasibility are not taken into consideration. The missing study of actual available lands and technologically reachable offshore sites prevent from adopting a methodology similar to the EEA's 2009 report (EEA, 2009), and thus from assessing actual wind power that could have been harvested through the thirty-one years of the database, with intermittency and variability aspects taken in to account.

In spite of these limitations, relevant conclusions have been reached. Overall, the availability of onshore wind power is low and is highly intermittent, while offshore locations show a high degree of persistence. Even if the benefits of wide interconnection between wind farms thorough Europe is limited, for the onshore locations of strongest wind power—primarily over northern coastlines as well as the United Kingdom, Ireland and Iceland—the evidence indicates that intermittency can be reduced by aggregation and interconnection of wind-power installations.

Acknowledgments

The authors gratefully acknowledge the financial support for this work provided by the MIT Joint Program on the Science and Policy of Global Change through a consortium of industrial sponsors and Federal grants, including U.S. Department of Energy grant DE-FG02-94ER61937. In addition, the authors would like to thank Mr. Hervé Le Treut and Prof. Ronald G. Prinn, who have given the opportunity to Alexandra Cosseron, French graduate student from Ecole Polytechnique and Ecole des Mines de Paris, to join the MIT Joint Program on the Science and Policy of Global Change for this work.

REFERENCES

- Archer, C.L., 2005: Evaluation of global wind power. *Journal of Geophysical Research*, 110(D12): 1–20, doi: 10.1029/2004JD005462.
- Archer, C.L., and M.Z. Jacobson, M. Z., 2007. Supplying Baseload Power and Reducing Transmission Requirements by Interconnecting Wind Farms. *Journal of Applied Meteorology and Climatology*, 46(11): 1701–1717, doi: 10.1175/2007JAMC1538.1. (<http://journals.ametsoc.org/doi/abs/10.1175/2007JAMC1538.1>).
- Cosseron, A., U.B. Gunturu, and C.A. Schlosser, 2013: Characterization of the wind power resource over Europe and its intermittency. *Energy Procedia*, 40(May2011): 58–66.

- Cox, J., 2009: Impact of Intermittency: How Wind Variability could change the shape of the British and Irish Electricity Markets—Summary report July 2009. *Technical Report July 2009*, Poyry Company.
- EEA (European Environment Agency), 2009: Europe's onshore and offshore wind energy potential—An assessment of environmental and economic constraints. *Technical Report 6*, (<http://www.eea.europa.eu/publications/europes-onshore-and-offshore-wind-energy-potential>).
- Elliot, D.L., C.G. Holladay, W.R. Barchet, H.P. Foote, and W.F. Sandusky, 1987: *Wind Energy Resource Atlas of the United States*. DOE/CH 10093-4, Solar Energy Research Institute: Golden, Colorado.
- Estanqueiro, A.I., 2008: Impact of Wind Generation Fluctuations in the Design and Operation of Power Systems. 7th International Workshop on Large Scale Integration of Wind Power and on Transmission Networks for Offshore Wind Farms, May 26–27, Madrid, Spain (http://repositorio.ineg.pt/bitstream/10400.9/931/1/Paper85_Fluctuations_VF1.pdf).
- European Commission, 2009: Directive 2009/28/EC of the European Parliament and of the council of 23 April 2009 on the promotion of the use of energy from renewable sources and amending and subsequently repealing Directives 2001/77/EC and 2003/30/EC. *Official Journal of the European Union*.
- Gunturu, U.B., and C.A. Schlosser, 2012: Characterization of Wind Power Resource in the United States. *Atmospheric Chemistry and Physics*, 12: 9687–9702.
- Gunturu, U.B., and C.A. Schlosser, 2011: Characterization of Wind Power Resource in the United States and its Intermittency. MIT JPSPGC Report 209, December, 65 p. (http://globalchange.mit.edu/files/documents/MITJPSPGC_Rpt209.pdf).
- Gustavson, M.R., 1979: Limits to Wind Power Utilization. *Science*, 204(4388): 13–17.
- Hennessey, J.P., 1977: Some Aspects of Wind Power Statistics. *Journal of Applied Meteorology*, 16(2): 119–128.
- Holttinen, H., 2005: Impact of hourly wind power variations on the system operation in the Nordic countries. *Wind Energy*, 8(2): 197–218, doi: 10.1002/we.143.
- Holttinen, H., M., Milligan, B. Kirby, T. Acker, V. Neimane, and T. Molinski, 2008: Using Standard Deviation as a Measure of Increased Operational Reserve Requirement for Wind Power. *Wind Engineering*, 32(4): 355–377. doi: 10.1260/0309-524X.32.4.355.
- Kiss, P., and I.M. Janosi, 2008: Limitations of wind power availability over Europe: a conceptual study. *Nonlinear Processes in Geophysics*, 15: 803–813.
- Larsén, X. G., and J. Mann, 2009: Extreme Winds from the NCEP/NCAR Reanalysis Data. *Wind Energy*, 12(6): 556–573, doi: 10.1002/we.318.
- Lund, H., 2005: Large-scale integration of wind power into different energy systems. *Energy*, 30(13): 2402–2412. doi: 10.1016/j.energy.2004.11.001.
- Rienecker, M.M., M.J. Suarez, R. Gelaro, R. Todling, J. Bacmeister, E. Liu, M.G. Bosilovich, S.D., Schubert, L. Takacs, G. Kim, S. Bloom, J. Chen, D. Collins, A. Conaty, A. da Silva, W. Gu, J. Joiner, R.D. Koster, R. Lucchesi, A. Molod, T. Owens, S. Pawson, P. Pegion,

- C.R. Redder, R. Reichle, F.R. Robertson, A.G. Ruddick, M. Sienkiewicz, and J. Woollen, 2011: MERRA: NASA's Modern-Era Retrospective Analysis for Research and Applications. *Journal of Climate*, 24(14):3624–3648, doi:10.1175/JCLI-D-11-00015.1.
- Stull, R.B., 1988: *An Introduction to Boundary Layer Meteorology*. Springer. ISBN 978-90-277-2769-5.
- Troen, I., and E.L. Petersen, 1989: *European Wind Atlas*. Risø National Laboratory. ISBN 87-550-1482-8.
- Vestas, 2012a: *V112-3.0MW Onshore Brochure*. Vestas.
- Vestas, 2012b: *V112-3.0MW Offshore Brochure*. Vestas.
- Wilkes, J., J. Moccia, and M. Dragan, 2012: *Wind in power—2011 European statistics*. Technical Report, European Wind Energy Association (EWEA).

REPORT SERIES of the MIT Joint Program on the Science and Policy of Global Change

FOR THE COMPLETE LIST OF JOINT PROGRAM REPORTS:
<http://globalchange.mit.edu/pubs/all-reports.php>

211. **Emissions Pricing to Stabilize Global Climate** *Bosetti et al.* March 2012
212. **Effects of Nitrogen Limitation on Hydrological Processes in CLM4-CN** *Lee & Felzer* March 2012
213. **City-Size Distribution as a Function of Socio-economic Conditions: An Eclectic Approach to Down-scaling Global Population** *Nam & Reilly* March 2012
214. **CliCrop: a Crop Water-Stress and Irrigation Demand Model for an Integrated Global Assessment Modeling Approach** *Fant et al.* April 2012
215. **The Role of China in Mitigating Climate Change** *Paltsev et al.* April 2012
216. **Applying Engineering and Fleet Detail to Represent Passenger Vehicle Transport in a Computable General Equilibrium Model** *Karplus et al.* April 2012
217. **Combining a New Vehicle Fuel Economy Standard with a Cap-and-Trade Policy: Energy and Economic Impact in the United States** *Karplus et al.* April 2012
218. **Permafrost, Lakes, and Climate-Warming Methane Feedback: What is the Worst We Can Expect?** *Gao et al.* May 2012
219. **Valuing Climate Impacts in Integrated Assessment Models: The MIT IGSM** *Reilly et al.* May 2012
220. **Leakage from Sub-national Climate Initiatives: The Case of California** *Caron et al.* May 2012
221. **Green Growth and the Efficient Use of Natural Resources** *Reilly* June 2012
222. **Modeling Water Withdrawal and Consumption for Electricity Generation in the United States** *Strzepek et al.* June 2012
223. **An Integrated Assessment Framework for Uncertainty Studies in Global and Regional Climate Change: The MIT IGSM** *Monier et al.* June 2012
224. **Cap-and-Trade Climate Policies with Price-Regulated Industries: How Costly are Free Allowances?** *Lanz and Rausch* July 2012.
225. **Distributional and Efficiency Impacts of Clean and Renewable Energy Standards for Electricity** *Rausch and Mowers* July 2012.
226. **The Economic, Energy, and GHG Emissions Impacts of Proposed 2017–2025 Vehicle Fuel Economy Standards in the United States** *Karplus and Paltsev* July 2012
227. **Impacts of Land-Use and Biofuels Policy on Climate: Temperature and Localized Impacts** *Hallgren et al.* August 2012
228. **Carbon Tax Revenue and the Budget Deficit: A Win-Win Solution?** *Sebastian Rausch and John Reilly* August 2012
229. **CLM-AG: An Agriculture Module for the Community Land Model version 3.5** *Gueneau et al.* September 2012
230. **Quantifying Regional Economic Impacts of CO₂ Intensity Targets in China** *Zhang et al.* September 2012
231. **The Future Energy and GHG Emissions Impact of Alternative Personal Transportation Pathways in China** *Kishimoto et al.* September 2012
232. **Will Economic Restructuring in China Reduce Trade-Embodied CO₂ Emissions?** *Qi et al.* October 2012
233. **Climate Co-benefits of Tighter SO₂ and NO_x Regulations in China** *Nam et al.* October 2012
234. **Shale Gas Production: Potential versus Actual GHG Emissions** *O'Sullivan and Paltsev* November 2012
235. **Non-Nuclear, Low-Carbon, or Both? The Case of Taiwan** *Chen* December 2012
236. **Modeling Water Resource Systems under Climate Change: IGSM-WRS** *Strzepek et al.* December 2012
237. **Analyzing the Regional Impact of a Fossil Energy Cap in China** *Zhang et al.* January 2013
238. **Market Cost of Renewable Jet Fuel Adoption in the United States** *Winchester et al.* January 2013
239. **Analysis of U.S. Water Resources under Climate Change** *Blanc et al.* February 2013
240. **Protection of Coastal Infrastructure under Rising Flood Risk** *Lickley et al.* March 2013
241. **Consumption-Based Adjustment of China's Emissions-Intensity Targets: An Analysis of its Potential Economic Effects** *Springmann et al.* March 2013
242. **The Energy and CO₂ Emissions Impact of Renewable Energy Development in China** *Zhang et al.* April 2013
243. **Integrated Economic and Climate Projections for Impact Assessment** *Paltsev et al.* May 2013
244. **A Framework for Modeling Uncertainty in Regional Climate Change** *Monier et al.* May 2013
245. **Climate Change Impacts on Extreme Events in the United States: An Uncertainty Analysis** *Monier and Gao* May 2013
246. **Probabilistic Projections of 21st Century Climate Change over Northern Eurasia** *Monier et al.* July 2013
247. **What GHG Concentration Targets are Reachable in this Century?** *Paltsev et al.* July 2013
248. **The Energy and Economic Impacts of Expanding International Emissions Trading** *Qi et al.* August 2013
249. **Limited Sectoral Trading between the EU ETS and China** *Gavard et al.* August 2013
250. **The Association of Large-Scale Climate Variability and Teleconnections on Wind Resource over Europe and its Intermittency** *Kriesche and Schlosser* September 2013
251. **Regulatory Control of Vehicle and Power Plant Emissions: How Effective and at What Cost?** *Paltsev et al.* October 2013
252. **Synergy between Pollution and Carbon Emissions Control: Comparing China and the U.S.** *Nam et al.* October 2013
253. **An Analogue Approach to Identify Extreme Precipitation Events: Evaluation and Application to CMIP5 Climate Models in the United States** *Gao et al.* November 2013
254. **The Future of Global Water Stress: An Integrated Assessment** *Schlosser et al.* January 2014
255. **The Mercury Game: Evaluating a Negotiation Simulation that Teaches Students about Science–Policy Interactions** *Stokes and Selin* January 2014
256. **The Potential Wind Power Resource in Australia: A New Perspective** *Hallgren et al.* February 2014
257. **Equity and Emissions Trading in China** *Zhang et al.* February 2014
258. **Characterization of the Wind Power Resource in Europe and its Intermittency** *Cosseron et al.* March 2014